

Cover Page



Universiteit Leiden



The handle <http://hdl.handle.net/1887/25491> holds various files of this Leiden University dissertation

Author: Vorst, Joost van der

Title: Near-infrared fluorescence-guided surgery : pre-clinical validation and clinical translation

Issue Date: 2014-05-01

Chapter 13

Intraoperative near-infrared fluorescence imaging of parathyroid adenomas using low-dose methylene blue

van der Vorst JR¹, Schaafsma BE¹, Verbeek FP, Swijnenburg RJ, Hutteman M,
Hamming JF, Kievit J, Frangioni JV, van de Velde CJ, Vahrmeijer AL

¹Both authors contributed equally to this work and share first authorship.

Head Neck. 2013 May 29

ABSTRACT

Background

Intraoperative identification of parathyroid adenomas can be challenging. We hypothesized that low-doses methylene blue (MB) and near-infrared fluorescence (NIRF) imaging could be used to identify parathyroid adenomas intraoperatively.

Material and Methods

MB was injected intravenously after exploration at a dose of 0.5 mg/kg into 12 patients who underwent parathyroid surgery. NIRF imaging was performed using the Mini-FLARE™ imaging system.

Results

In 10 of 12 patients, histology confirmed a parathyroid adenoma. In 9 of these patients, NIRF could clearly identify the parathyroid adenoma during surgery. Seven of these 9 patients had a positive preoperative ^{99m}Tc-sestamibi SPECT scan. Importantly, in two patients, parathyroid adenomas could be identified only using NIRF.

Conclusion

This is the first study to show that low-dose MB can be used as NIRF tracer for identification of parathyroid adenomas, and suggests a correlation with preoperative ^{99m}Tc-sestamibi SPECT scanning.

INTRODUCTION

Primary hyperparathyroidism is a common endocrine disorder caused by overproduction of parathyroid hormone (PTH) by adenomatous or hyperplastic parathyroid glands. In hyperparathyroidism patients, resection of these glands is the only curative treatment. The wide variability of the anatomical location, shape, and number of parathyroid glands makes successful parathyroid surgery challenging. Various preoperative imaging modalities contribute to detailed surgical planning, which is particularly important when using a minimally invasive surgical approach.¹⁻³ Currently, a combination of a cervical ultrasonography (US) and a ^{99m}Tc-sestamibi planar scan, whether or not combined with a single-photon emission computed tomography (SPECT) 3D scan, is most often used for preoperative localization. However, only few intraoperative imaging modalities are available. Despite that the current success rate of parathyroidectomy exceeds 95% without any intraoperative imaging adjuncts in the hands of experienced surgeons,^{1,4} intraoperative imaging tools could aid in the localization of difficult localized parathyroid adenoma and in addition possibly reduce time of surgery.⁵

For intraoperative localization, radioguided parathyroidectomy using ^{99m}Tc-sestamibi has been reported.^{6,7} This technique, however, lacks real-time visual information. High-dose methylene blue (MB), used as a blue dye, was introduced by Dudley and colleagues in 1971⁸ for the intraoperative identification of parathyroid adenomas by a simple peripheral infusion.^{6,9,10} reporting sensitivity and specificity of 79% and 93% respectively.^{10,11} However, a major disadvantage of using MB is that the high dose (7.5 mg/kg) required for visualization of blue color by the human eye brings a substantial risk of serious adverse events, such as toxic metabolic encephalopathy.¹² A different, recently introduced, technique is the use of visible fluorescence and aminolevulinic acid (ALA) to identify parathyroid glands, which was successfully tested in clinical studies.¹³⁻¹⁵ However, ALA can cause phototoxic reactions for which patients have to be shielded from direct light exposure for 48 hours. Furthermore, sub-surface detectability using ALA is minimal due to high absorption and scatter of visible light in living tissue. Therefore, novel and improved intraoperative imaging modalities to aid the surgeon in localization of the parathyroid glands are needed during parathyroid surgery.

Near-infrared (NIR) fluorescence imaging is a promising technique that also facilitates intraoperative, real-time, visual information.¹⁶⁻¹⁸ This technique is based on the use of exogenous NIR fluorescent contrast agents that can be detected

by intraoperative imaging systems to visualize specific tissues. Advantage of this technique are its high sensitivity and high tissue penetration of approximately 5 millimeters. As such, it has wide applications, including sentinel lymph node mapping in several tumor types.¹⁹⁻²² MB, which was used for parathyroid adenoma identification as stated above, has the advantageous property that it becomes a moderate-strength fluorophore emitting at ≈ 700 nm when diluted to levels that are almost undetectable to the human eye. When lower doses of MB can still provide clear identification of parathyroid adenomas using NIR fluorescence, this could significantly reduce the risk for adverse events.²³ The aim of this study was to assess feasibility of using low-dose MB for intraoperative NIR fluorescence-guided detection of parathyroid adenomas. Furthermore, the concordance between preoperative ^{99m}Tc-sestamibi-SPECT scanning and intraoperative NIR fluorescence was preliminarily assessed.

MATERIAL AND METHODS

Clinical Study

This study was approved by the Medical Ethics Committee of the Leiden University Medical Center and was performed in accordance with the ethical standards of the Helsinki Declaration of 1975. All patients planning to undergo a resection of a parathyroid adenoma for primary hyperparathyroidism or parathyromatosis were eligible for participation in the study. Exclusion criteria were pregnancy or lactation, the use of serotonin reuptake inhibitors, serotonin, and noradrenalin reuptake inhibitors and/or tricyclic antidepressants, severe renal failure, G6PD-deficiency, or an allergy to MB. All patients gave informed consent and were anonymized. Patients received standard of care diagnostic work-up, which for our center implied a preoperative ^{99m}Tc-sestamibi-SPECT, which was sometimes combined with a low-dose computed tomography (CT) scan for preoperative surgical planning. If indicated a preoperative cervical US was performed. After subplatysmal dissection, retraction, draping and initial surgical exploration of the suspected parathyroid adenoma in the neck region, 0.5 mg/kg of MB (concentration 10 mg/ml) was infused intravenously over 5 min. Subsequently, NIR fluorescence imaging of the neck region was performed using the Mini-FLARE NIR fluorescence imaging system, which has been described previously.²⁰ In one patient a thoracotomy was performed after SPECT-CT localization of the parathyroid adenoma in pericardium.

After resection of the putative parathyroid adenoma, an intraoperative PTH assay was performed. Post-operative histopathological examination was obtained, which served as gold standard for parathyroid adenoma identification. Parathyroid tissue was snap frozen and sectioned at 10 μm for fluorescence microscopy.

Fluorescence Microscopy

Snap frozen tissue was sectioned at 10 μm for fluorescence microscopy, which was performed on a Zeiss LSM 700 Confocal Laser Scanning Microscope and a Zeiss HBO 100 Microscope Illuminating System (Jena, Germany) using a 633 nm laser for excitation and a 650 nm high pass emission filter. Subsequently, tissue sections were stained with hematoxylin and eosin (H&E).

Statistical Analysis

For statistical analysis, SPSS statistical software package (Version 16.0, Chicago, IL) was used. Signal-to-background ratios were calculated by dividing the fluorescent signal in the parathyroid adenoma by fluorescent signal of surrounding healthy tissue. Patient age and body mass index (BMI) were reported in median and range and signal-to-background was reported in mean and standard deviation. To compare fluorescent signal in the parathyroid adenoma with fluorescent signal in the thyroid gland, the independent-sample *t* test was used. $P < 0.05$ was considered significant.

RESULTS

Study Subjects

Patient characteristics and histological results of the 12 patients included are listed in Table 1. Median patient age was 58 years (range 17 – 78 years), median BMI was 26 (range 18 – 34 kg/m^2). Eleven patients were planned for surgery for primary hyperparathyroidism and 1 patient suffered from parathyromatosis. Prior to the study, one patient underwent a total thyroid resection, one patient a parathyroid adenoma resection, and one patient had undergone previous parathyroid surgery 3 times as well as a thymectomy. During the current study, a resection of the putative diseased tissue was performed in all patients. Histopathological examination showed a solitary parathyroid adenoma in 7 patients, two parathyroid adenomas in 1 patient, small parathyroid fragments in 1 patient, a parathyroid carcinoma in

1 patient and a thyroid carcinoma with a synchronous parathyroid adenoma in 2 patients. Average maximum diameter of the resected lesions was 15.7 ± 8.7 mm.

Preoperative Imaging

In all patients, a preoperative ^{99m}Tc -sestamibi-SPECT scan was performed which was combined with a low-dose CT-scan in 10 patients. In 8 of 12 patients, the ^{99m}Tc -sestamibi-SPECT scan could identify the parathyroid adenoma. In 9 of 12 patients a preoperative ultrasonography was performed, which was positive in 4 patients. Preoperative imaging results are summarized in Table 2.

Intraoperative NIR Fluorescence Imaging

Intraoperative NIR fluorescent guidance was provided by the Mini-FLARE imaging system and MB, which clearly identified a hyperparathyroid adenoma in 9 patients (Figs. 1 and 2). Of these patients, the average signal-to-background ratio (SBR) was 6.1 ± 4.1 . Importantly, in 2 of these 9 NIR fluorescence-positive patients, the parathyroid adenoma was not identified using the ^{99m}Tc -sestamibi-SPECT scan or preoperative ultrasound. In 3 of 12 patients, no intraoperative fluorescent signal could be detected. In two of these patients, no parathyroid adenoma was found during histological examination (parathyromatosis and a necrotic parathyroid carcinoma). In one patient a normal parathyroid adenoma, which contained extensive fibrosis and bleeding, was identified. In other words, in 9 of 10 patients diagnosed with a parathyroid adenoma, the adenoma could be identified using NIR fluorescence. No significant difference was observed between parathyroid fluorescence and thyroid fluorescence (322.6 ± 272.1 vs. 220.2 ± 186.7 , $P = 0.25$). During the course of the study, no adverse events were observed.

In 9 of 12 patients, preoperative results using ^{99m}Tc -sestamibi overlapped with intraoperative NIR fluorescence. In 1 patient in whom the ^{99m}Tc -sestamibi-scan was positive, no fluorescent signal could be obtained. This patient was found to have a parathyroid carcinoma. In 2 patients in whom the ^{99m}Tc -sestamibi-scan was negative, NIR fluorescence could identify the parathyroid adenoma. In 3 of 9 patients in whom an ultrasonography was performed, results overlapped with NIR fluorescence. The overlap between different imaging modalities and the location of the parathyroid glands is schematically shown in Figure 3.

Table 1 – Patient and surgical characteristics

Subject	Gender	Age	BMI	Disease	Previous treatment	Preop calcium (mmol/L)	Preop PTH (pmol/L)	Surgical procedure	Histology	Max diameter (mm)
1	F	67	34	PH	No	1.48	17.7	PAR right, thyroid biopsy, thyroidal cystectomy	Parathyroid adenoma	8
2	F	78	24	PH	Total thyroid resection	NA	17.8	PAR right, resection of thyroidal nodule right, parathyroid gland resection left	Parathyroid adenoma	9
3	F	58	27	PH	PAR	2.98	NA	Intermediastinal PAR, thymectomy	Parathyroid adenoma	20
4	M	48	31	PT	Parathyroid surgery (3x); thymectomy	2.76	8.7	Resection of 8 tissue fragments	Parathyromatosis	fragments < 21 mm
5	F	17	24	PH	No	2.71	11.4	Thyroid biopsy, subtotal parathyroidectomy	Parathyroid adenoma	11
6	M	58	26	PH	No	3.15	9.6	PAR left, resection suspected lymph nodes, resection left thyroid	Parathyroid adenoma, thyroid carcinoma	30
7	F	44	30	PH	No	2.7	231	PAR right, hemithyroidectomy right	Parathyroid carcinoma	30
8	F	60	23	PH	No	2.59	16.7	PAR left	Parathyroid adenoma	7
9	M	78	23	PH	No	2.78	23.8	PAR right	Parathyroid adenoma	22
10	F	52	33	PH	No	2.77	34.3	PAR right, hemithyroidectomy right, resection suspected nodes left, thymectomy	Parathyroid adenoma, (2) thyroid carcinoma	8;4
11	F	49	18	PH	No	3.00	47.7	PAR retrosternal	Parathyroid adenoma	15
12	F	64	32	PH	No	2.59	14.5	PAR left	Parathyroid adenoma	15

BMI: Body-mass index; Preop: preoperative, PH: primary hyperparathyroidism; PT: parathyromatosis; PAR: parathyroid adenoma resection

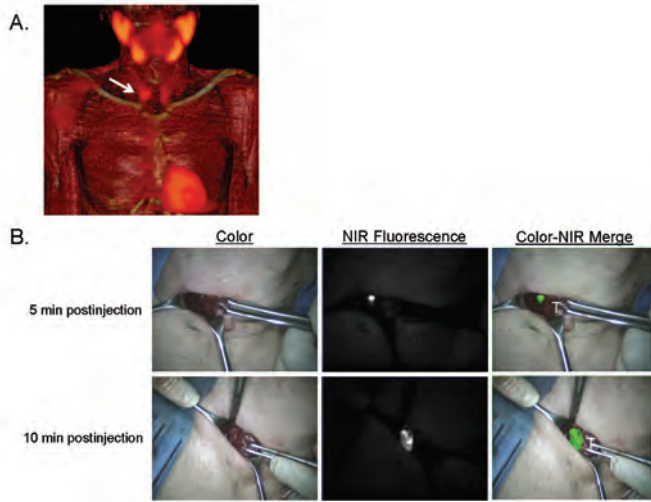


Figure 1 – Preoperative surgical planning and intraoperative NIR fluorescence-guided resection of a parathyroid adenoma located in the neck:

A: 3D SPECT-CT image 2 h postinjection of ^{99m}Tc -sestamibi with visualization of a parathyroid adenoma located at the right side of the neck (arrow).

B: During minimally-invasive parathyroid surgery, a parathyroid adenoma is identified using NIR fluorescence imaging, 5 and 10 minutes postinjection of 0.5 mg/kg MB. T= thyroid tissue.

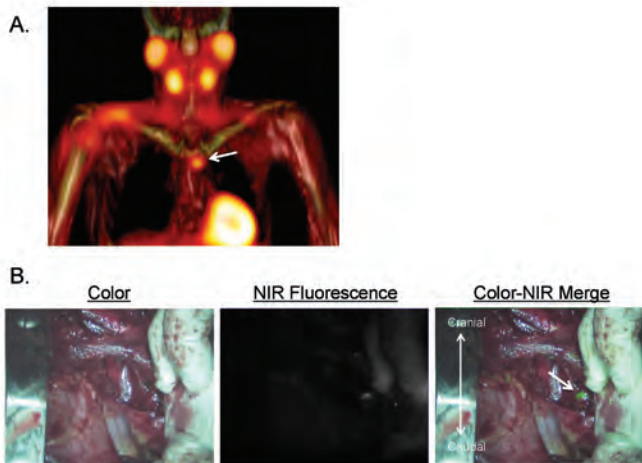


Figure 2 – Preoperative surgical planning and intraoperative NIR fluorescence-guided resection of a parathyroid adenoma located in the mediastinum:

A: 3D SPECT-CT image 2 h postinjection of ^{99m}Tc -sestamibi with visualization of a parathyroid adenoma located paratracheally in the mediastinum (arrow).

B: A parathyroid adenoma located paratracheally in the mediastinum is identified using NIR fluorescence imaging, 10 minutes postinjection of 0.5 mg/kg MB.

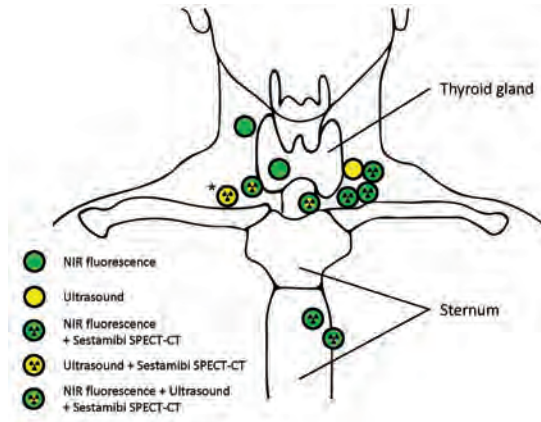


Figure 3 – Schematic overview of parathyroid adenoma location and corresponding detection methods: Shown is the location of all parathyroid adenomas (N = 10) and one parathyroid carcinoma (N = 1, Asterix) and corresponding imaging modalities with which they were identified. The patient with parathyromatosis was excluded from this scheme.

Fluorescence Microscopy

700 NIR fluorescence signal of methylene blue was located within oncocytic cells as confirmed using H&E staining of the same specimen (Fig. 4).

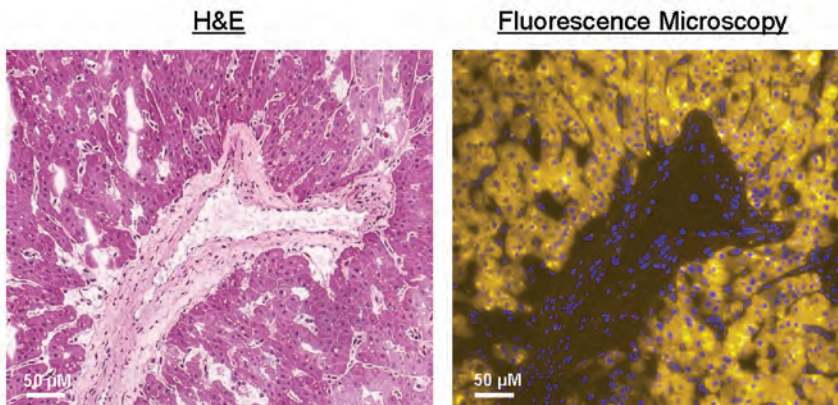


Figure 4 – Histopathological evaluation and fluorescence microscopy:

Shown are 40X H&E staining (left) of the resected specimen, which shows oncocytic cells with monotone round nuclei surrounding a blood vessel. The right image shows the same section stained with 4',6-diamidino-2-phenylindole (DAPI) nuclear staining (blue), with the 700 nm NIR fluorescence from MB pseudo-colored in yellow. The NIR fluorescent signal is located in the oncocytic cells.

Table 2 –Identification of parathyroid adenomas

Subject #	Sestamibi-SPECT-CT	Preoperative Ultrasound	PTH decrease Post-resection	NIR fluorescence detection	SBR
1	-	-	+	+	5.48
2	+	-	+	+	9.59
3	+	-	+	+	4.37
4	-	-	-	-	n/a
5	+*	NP	+	+	2.68
6	-	+	+	-	n/a
7	+*	+	+	-	n/a
8	+	+	+	+	4.45
9	+	+	+	+	5.50
10	-	-	+	+	1.91
11	+	NP	+	+	5.21
12	+	NP	+	+	15.33

PTH: parathyroid hormone; n/a: not applicable; NIR: Near-infrared; NP: Not performed; SBR: signal-to-background ratio; *: SPECT without CT was performed

DISCUSSION

The primary objective of the current study was to test the feasibility of NIR fluorescence with low-dose MB (0.5 mg/kg; 15 times lower than the dose used for macroscopic identification) to identify parathyroid adenomas during surgery. Furthermore, concordance between ^{99m}Tc-sestamibi SPECT and intraoperative NIR fluorescence imaging results was assessed. Two patients were not diagnosed with a parathyroid adenoma. A clear identification of parathyroid adenomas using NIR fluorescence was found in 9 of 10 patients who were histologically diagnosed with a parathyroid adenoma. Furthermore, a high overlap between imaging results of ^{99m}Tc-sestamibi SPECT and NIR fluorescence was observed.

In 3 of 12 patients, no clear identification of the lesion could be obtained using NIR fluorescence. In one of these patients, histopathological examination revealed a parathyroid carcinoma. This carcinoma was described as a highly necrotic lesion, which presumably hampered MB uptake in this lesion. Alternatively, carcinoma may not take up MB like benign lesions. One patient suffered from extended cervical parathyromatosis and in this patient all parathyroid glands were already surgically removed in the past. In this patient, the parathyroid tissue could not be demarcated from the surrounding tissue, however no adenomas were

present. In one patient with a large parathyroid adenoma, in whom no adequate SBR could be obtained, the adenoma contained extensive fibrosis and bleeding. The extensive fibrosis and bleeding could have hampered uptake of MB in the adenoma, which might also explain the negative ^{99m}Tc -sestamibi SPECT scan.

A potential pitfall using the technology we describe is the background signal in the thyroid gland. It is known from data acquired in patients undergoing ^{99m}Tc -sestamibi radioscintigraphy that adenomatous and hyperplastic parathyroid tissue show more avid uptake of ^{99m}Tc -sestamibi, although initially this activity can be obscured by uptake from the adjacent thyroid gland. The observation that abnormal parathyroid tissue commonly retains ^{99m}Tc -sestamibi longer than thyroid gland tissue has led to the widespread use of delayed imaging.²⁴ Therefore, an early (15-30 min.) and delayed (2-3 hr.) imaging sequence is performed. Furthermore, a window of 4 hours between administration and imaging was also used in the clinical studies that used ALA for parathyroid identification.^{13,15} In the current study, high thyroid gland uptake of MB was observed. We hypothesize that a similar delayed imaging protocol could improve the contrast between thyroid gland and parathyroid gland tissue.

Although conventional preoperative imaging modalities (^{99m}Tc -sestamibi scan and US) achieve an accurate preoperative localization of the adenoma in most cases (sensitivity approximately 80% for both techniques), intraoperative identification can be challenging.²⁵ In this perspective, time needed to intraoperatively localize the adenoma may decrease using NIR fluorescence and MB. The comparable biological characteristics of MB and sestamibi, both lipophilic and cationic, resulted in a high concordance between the outcome of ^{99m}Tc -sestamibi scans and NIR fluorescence detection in 7 of 9 patients in the current study. The results of the ^{99m}Tc -sestamibi SPECT-CT may therefore help predict those patients that will most likely benefit from NIR fluorescence intraoperative imaging.

The current study was the first to show that low-dose MB and NIR fluorescence can be used for the intraoperative detection of parathyroid adenomas after a simple peripheral infusion. Though this technique will not replace the detailed and thorough anatomical knowledge and experience of surgeons, which are the key factors for successful parathyroidectomy. Due to the significantly lower doses MB that can be used, this technique can provide valuable additional information during surgery in a safe manner, provided that proper exclusion criteria are followed. However, optimization of MB dose, timing of injection, clinical outcome and patient benefit need to be studied in larger clinical trials.

REFERENCES

1. Udelsman R. Six hundred fifty-six consecutive explorations for primary hyperparathyroidism. *Ann Surg* 2002; 235:665-670.
2. Grant CS, Thompson G, Farley D et al. Primary hyperparathyroidism surgical management since the introduction of minimally invasive parathyroidectomy: Mayo Clinic experience. *Arch Surg* 2005; 140:472-478.
3. Lew JI, Solorzano CC. Surgical management of primary hyperparathyroidism: state of the art. *Surg Clin North Am* 2009; 89:1205-1225.
4. Norman J, Lopez J, Politz D. Abandoning unilateral parathyroidectomy: why we reversed our position after 15,000 parathyroid operations. *J Am Coll Surg* 2012; 214:260-269.
5. Patel CN, Salahudeen HM, Lansdown M et al. Clinical utility of ultrasound and 99mTc sestamibi SPECT/CT for preoperative localization of parathyroid adenoma in patients with primary hyperparathyroidism. *Clin Radiol* 2010; 65:278-287.
6. Harrison BJ, Triponez F. Intraoperative adjuncts in surgery for primary hyperparathyroidism. *Langenbecks Arch Surg* 2009; 394:799-809.
7. Flynn MB, Bumpous JM, Schill K et al. Minimally invasive radioguided parathyroidectomy. *J Am Coll Surg* 2000; 191:24-31.
8. Dudley NE. Methylene blue for rapid identification of the parathyroids. *Br Med J* 1971; 3:680-681.
9. Han N, Bumpous JM, Goldstein RE et al. Intra-operative parathyroid identification using methylene blue in parathyroid surgery. *Am Surg* 2007; 73:820-823.
10. Orloff LA. Methylene blue and sestamibi: complementary tools for localizing parathyroids. *Laryngoscope* 2001; 111:1901-1904.
11. Raffaelli M. Systematic review of intravenous methylene blue in parathyroid surgery (*Br J Surg* 2012; 99: 1345-1352). *Br J Surg* 2012; 99:1352.
12. Kartha SS, Chacko CE, Bumpous JM et al. Toxic metabolic encephalopathy after parathyroidectomy with methylene blue localization. *Otolaryngol Head Neck Surg* 2006; 135:765-768.
13. Prosst RL, Weiss J, Hupp L et al. Fluorescence-guided minimally invasive parathyroidectomy: clinical experience with a novel intraoperative detection technique for parathyroid glands. *World J Surg* 2010; 34:2217-2222.
14. Prosst RL, Gahlen J, Schnuelle P et al. Fluorescence-guided minimally invasive parathyroidectomy: a novel surgical therapy for secondary hyperparathyroidism. *Am J Kidney Dis* 2006; 48:327-331.
15. Prosst RL, Willeke F, Schroeter L et al. Fluorescence-guided minimally invasive parathyroidectomy: a novel detection technique for parathyroid glands. *Surg Endosc* 2006; 20:1488-1492.
16. Keereweer S, Kerrebijn JD, van Driel PB et al. Optical Image-guided Surgery-Where Do We Stand? *Mol Imaging Biol* 2010.
17. Frangioni JV. New technologies for human cancer imaging. *J Clin Oncol* 2008; 26:4012-4021.
18. Gioux S, Choi HS, Frangioni JV. Image-guided surgery using invisible near-infrared light: fundamentals of clinical translation. *Mol Imaging* 2010; 9:237-255.
19. Hutteman M, Choi HS, Mieog JS et al. Clinical Translation of Ex Vivo Sentinel Lymph Node Mapping for Colorectal Cancer Using Invisible Near-Infrared Fluorescence Light. *Ann Surg Oncol* 2010; Epub ahead of print.
20. Mieog JS, Troyan SL, Hutteman M et al. Towards Optimization of Imaging System and Lymphatic Tracer for Near-Infrared Fluorescent Sentinel Lymph Node Mapping in Breast Cancer. *Ann Surg Oncol* 2011; 18:2483-2491.
21. Hutteman M, van der Vorst JR, Gaarenstroom KN et al. Optimization of near-infrared fluorescent sentinel lymph node mapping for vulvar cancer. *Am J Obstet Gynecol* 2011.
22. Crane LM, Themelis G, Pleijhuis RG et al. Intraoperative Multispectral Fluorescence Imaging for the Detection of the Sentinel Lymph Node in Cervical Cancer: A Novel Concept. *Mol Imaging Biol* 2010.
23. Majithia A, Stearns MP. Methylene blue toxicity following infusion to localize parathyroid adenoma. *J Laryngol Otol* 2006; 120:138-140.

24. Taillefer R, Boucher Y, Potvin C et al. Detection and localization of parathyroid adenomas in patients with hyperparathyroidism using a single radionuclide imaging procedure with technetium-99m-sestamibi (double-phase study). *J Nucl Med* 1992; 33:1801-1807.
25. Cheung K, Wang TS, Farrokhyar F et al. A meta-analysis of preoperative localization techniques for patients with primary hyperparathyroidism. *Ann Surg Oncol* 2012; 19:577-583.

